A Combined Method for Dielectric Waveguides Using the Finite-Element Technique and the Surface Integral Equations Method

CHING-CHUAN SU

Abstract—**A combined method employing a finite-element technique in the H_x-H_y formulation and the surface integral equations method is proposed to treat the propagation characteristics of inhomogeneous waveguides with single or multiple claddings. The significant features of this combined method are that it does not suffer from any kind of spurious modes, which have been troublesome in applying the finite-element technique to waveguides and it is also capable of treating the cutoff frequencies of arbitrarily shaped, inhomogeneous dielectric waveguides with a single cladding, which is perhaps original. Furthermore, the proposed method is convenient in treating propagation constants close to cutoff and in handling coupled waveguides. Numerical results of inhomogeneous elliptical waveguides, diffusion waveguides, and the corresponding directional couplers are presented, including the cutoff frequencies of the elliptical waveguides.**

I. Introduction

BY VIRTUE OF its flexibility in application, the finite-element technique has become an important tool in the numerical analysis of open or closed waveguides. However, a tedious problem prevailing in most applications of this technique is the occurrence of some nonphysical, or spurious modes, as noted in [1]–[6] and perhaps in [7] and [8]. In a previous investigation [9] for rotationally symmetric waveguides, where the E_z-H_z formulation is employed, an origin of spurious modes has been found and the locations of such modes have been predicted quantitatively. Although the case of inhomogeneous waveguides with arbitrary cross sections is much more complicated, the spurious modes occurring in the finite-element (or finite-difference) methods in the E_z-H_z formulation is believed to be due to the same origin: the denominator $[k_0^2\epsilon(x, y)-\beta^2]$ for expressing the transverse fields in terms of E_z and H_z, where k_0 denotes the free-space propagation constant, $\epsilon(x, y)$ is a relative permittivity distribution, and β is the propagation constant in the axial (z) direction. When β^2/k_0^2 becomes equal to some particular value of the permittivity distribution within a finite-element subregion, such a denominator will make some rows (corresponding to the nodes of that subregion) of matrix elements proportional to each other and thereby render the resultant matrix equation ill-conditioned. Accordingly, the number of such spurious modes will increase when the number of subregions increases or the permittivity distribution becomes complicated (away from a uniform distribution), which agrees with the observation in [4]. In view of this, a finite-element technique formulated in other fields (rather than the axial fields E_z and H_z) should be suitable. Among them, the H_x-H_y [10], the E_x-E_y [11], and the full H [5], [6] formulations have been proposed (although motivated by other purposes). Beside this kind of spurious modes, Konrad also discussed [12] another class of spurious modes that are caused by inadequate boundary conditions. The spurious modes in [5] and [6] where the full H formulation is employed seem to be a result of the approximate boundary conditions.

Beside the spurious modes, one major problem in the finite-element analysis of open waveguides is how to treat the infinite transverse cross section. One of the approaches is to impose an artificial zero boundary condition on the associated fields [2], [3], [7], [13]. This approach works when the actual fields decay considerably at the zero boundary. To obtain satisfactory results, such a boundary should be extended far away from the core region, which means that the computation effort will be increased. The second approach is to employ some kind of "infinite elements" which extend to infinity [5], [8]. Since the field behavior of such elements cannot be determined *a priori*, the fields therein should be modeled by some trial-and-error decay parameters to obtain reasonable results. The above two approaches involve difficulty in calculating the propagation constants near cutoff, since the fields penetrate deeply into the outer cladding medium. For the cases of inhomogeneous waveguides cladded by a single homogeneous region, a more rigorous approach is to incorporate some surface integrals as boundary conditions. Such surface integrals can be obtained from a finite-element formulation, as shown in [4] and [10]. The approach proposed by Oyamada and Okoshi [4] to treat the surface integrals together with the finite-element is to extend the core-cladding interface, within which the finite-element manipulation is to be applied, into a circular one. The fields on such a circular boundary are expanded in circular harmonics (the products of the modified Bessel functions and trigonometric functions) with coefficients to be determined. Such an approach is inefficient for an elongated waveguide and for coupled waveguides, since a large circular boundary

Manuscript received June 25, 1985; revised April 18, 1986.

The author is with the Department of Electrical Engineering, National Tsing Hua University, Hsinchu, Taiwan, Republic of China.

IEEE Log Number 8610505.

0018-9480/86/1100-1140$01.00 ©1986 IEEE

should be used to enclose the core region(s). Another approach to treat the combined formulation is proposed by Williams and Cambrell [10], where the surface integrals are treated by the moment method.[1] This approach, in some respects, is similar to the one employed in this investigation. However, with aid from the numerical procedure in the surface integral equations method [14], [15], we have generalized such a combined method so that it can handle the coupled waveguides efficiently, and that it can treat waveguides cladded by multiple homogeneous media (such as the diffusion waveguide). Furthermore, using Green's function at cutoff proposed in [14], the present method enables calculation of the cutoff frequencies of arbitrarily-shaped inhomogeneous waveguides with a single cladding, which to our knowledge is original.

In this investigation, the finite-element technique is formulated in transverse fields and is combined with the surface integral equations method. The main features of such a combined method are that it does not suffer from any kind of spurious mode, and that it is capable of treating a variety of dielectric waveguides, including coupled waveguides. The numerical procedure for such a combined method will be discussed in Sections II and IV. It should be stressed that even in treating coupled waveguides manipulation of the time-consuming finite-element is confined within the inhomogeneous region(s).

II. Surface Integral Equations Method

As shown in [14], for a homogeneous dielectric region with boundary C, any field component F (in rectangular coordinates) and its inward normal derivative dF/dn at the boundary can be related through a surface integral equation

$$\frac{A(\bar{r})}{2\pi}F(\bar{r}) = \oint_C F(\bar{r}')\frac{dG(\bar{r},\bar{r}')}{dn}\,d\bar{r}' - \oint_C G(\bar{r},\bar{r}')\frac{dF(\bar{r}')}{dn}\,d\bar{r}' \quad (1)$$

where G denotes Green's function for a transverse plane of the associated region, $A(\bar{r})$ is the interior angle of the boundary at $\bar{r}$, and $\oint$ denotes the Cauchy principal integral with the singularity at $\bar{r}' = \bar{r}$ removed. When the above integrals are discretized into matrix forms, one can express dF/dn explicitly in terms of F (in matrix form) after some matrix manipulations. When one employs such a method or other techniques to obtain explicit expressions for H_x and H_y for all the regions involved, one can determine propagation characteristics by enforcing the continuity requirement of E_z and H_z at all the boundaries encountered. Here, E_z and H_z can be expressed in terms of H_x and H_y and their normal derivatives as a consequence of Maxwell's equations (for details, see [14]). Cutoff frequencies of waveguides with a single cladding can be determined if one uses Green's function at cutoff for the cladding region as described in [14]. For unbounded waveguides (such as the diffusion waveguide), the corresponding infinite integrals in (1) are truncated, which has been justified in [15].

For a guiding structure containing some inhomogeneous regions, the corresponding explicit relations cannot be determined from (1) and must be treated otherwise. A promising method for such inhomogeneous regions is the finite-element technique, which is described in Sections III and IV. After the explicit relations for such regions are solved, the other procedures for obtaining the propagation characteristics are the same as just described.

It is noted that by using such a procedure, the propagation problem in this investigation is treated through an extraordinary eigenvalue problem, where the eigenvalues are determined in a searching procedure. The propagation problem given in [10] is formulated into an ordinary (but generalized) eigenvalue problem, where some iterative methods may be used. However, such a procedure cannot be applied to those waveguides with dispersive material and to those waveguides with multiple claddings.

III. Finite-Element Formulation

From Maxwell's equations, the magnetic fields of a guided mode satisfy the following source-free equation everywhere:

$$k_0^2\bar{H} - \nabla\times[\bar{\bar{\epsilon}}^{-1}\nabla\times\bar{H}] = 0. \quad (2)$$

On forming a dot product of the left-hand side of (2) with some arbitrary vector function $\bar{H}^c$ (independent of $\bar{H}$) and then integrating the scalar product over the entire space, one obtains

$$\int\{k_0^2\bar{H}\cdot\bar{H}^c - [\bar{\bar{\epsilon}}^{-1}\nabla\times\bar{H}]\cdot\nabla\times\bar{H}^c\}\,d\bar{r} = 0. \quad (3)$$

In writing (3), the vector identity $\nabla\cdot(\bar{A}\times\bar{B}) = (\nabla\times\bar{A})\cdot\bar{B} - \bar{A}\cdot(\nabla\times\bar{B})$ is used and the associated surface integral at the infinity is deleted since it plays no role in the actual treatment and indeed vanishes there. Equation (3) can be used to treat waveguides of general anisotropy. In this investigation we consider isotropic waveguides for which (2) reduces to

$$k_0^2\bar{H} - \nabla\times\frac{\nabla\times\bar{H}}{\epsilon(x,y)} = 0. \quad (4)$$

Employing the vector identity of $\nabla\times(A\bar{B}) = A(\nabla\times\bar{B}) + (\nabla A)\times\bar{B}$ and the relation $\nabla\cdot\bar{H} = 0$, (4) reduces to

$$k_0^2\epsilon(x,y)\bar{H} + \nabla^2\bar{H} - (\nabla\times\bar{H})\times\frac{\nabla\epsilon(x,y)}{\epsilon(x,y)} = 0 \quad (5)$$

from which one obtains, for an arbitrary function $\bar{H}^c$

$$\int\left\{k_0^2\epsilon\bar{H}\cdot\bar{H}^c + (\nabla^2\bar{H})\cdot\bar{H}^c - \left[(\nabla\times\bar{H})\times\frac{\nabla\epsilon}{\epsilon}\right]\cdot\bar{H}^c\right\}d\bar{r} = 0. \quad (6)$$

[1] We would like to point out that due to an erroneous application of the continuity of normal derivatives of associated fields at a permittivity discontinuity, the results in [10] happen to be scalar solutions, which is just a consequence pertaining to homogeneous waveguides.

For the propagation problem, all the fields are assumed to have fixed variation in the axial direction as $\exp(-j\beta z)$. Then, if $\bar{H}^c$ is chosen to be $\hat{x}H_x^c(x, y)e^{j\beta z}$ and $\hat{y}H_y^c(x, y)e^{j\beta z}$ (again, H_x^c and H_y^c are independent of H_x and H_y; and the use of $\exp(j\beta z)$ is to prevent (6) being identically zero and to make (6) independent of the variable z), one arrives at the following forms, respectively:

$$\int\left\{\left(k_0^2\epsilon-\beta^2\right)H_xH_x^c-\frac{\partial H_x}{\partial x}\frac{\partial H_x^c}{\partial x}-\frac{\partial H_x}{\partial y}\frac{\partial H_x^c}{\partial y}+\left(\frac{\partial H_y}{\partial x}-\frac{\partial H_x}{\partial y}\right)\frac{\partial \epsilon}{\partial y}\frac{1}{\epsilon}H_x^c\right\}dx\,dy=0 \quad (7a)$$

and

$$\int\left\{\left(k_0^2\epsilon-\beta^2\right)H_yH_y^c-\frac{\partial H_y}{\partial x}\frac{\partial H_y^c}{\partial x}-\frac{\partial H_y}{\partial y}\frac{\partial H_y^c}{\partial y}+\left(\frac{\partial H_x}{\partial y}-\frac{\partial H_y}{\partial x}\right)\frac{\partial \epsilon}{\partial x}\frac{1}{\epsilon}H_y^c\right\}dx\,dy=0. \quad (7b)$$

In writing (7), integration by parts has been used for those terms involving a second differentiation. From (7), it is noted that H_z has been uncoupled from H_x and H_y. On making a variation of (7a) and (7b) with respect to H_x^c and H_y^c, respectively, one obtains the previous governing equations in H_x and H_y implied in (5).

Similar formulas can be given for E_x and E_y; however, it is found on examining the results for a rotationally symmetric fiber for which rather accurate methods are available [16] that the E_x-E_y formulation yields results of less accuracy.

In a case where $\nabla\epsilon$ is small enough to be neglected, (7a) and (7b) become identical and H_x and H_y are uncoupled automatically. Such a situation is known as the scalar formulation. Because of the identity and the uncoupling the computation effort and the core storage of the scalar form can be reduced accordingly.

IV. Numerical Procedure for Finite-Element

In the finite-element treatment, the region of concern is divided into a number of subregions (or elements) within which the associated fields (H_x, H_y, H_x^c, and H_y^c) are expanded in some local basis functions with the expansion coefficients being the field nodal values. Thereafter, on making a variation of (7a) and (7b) with respect to H_x^c and H_y^c at all such nodes, one obtains $2N$ (N being the number of entire nodes) simultaneous equations in terms of H_x and H_y. Those equations obtained from taking the variation at the outermost nodes (the nodes on C_1 in Fig. 1) are incomplete and, hence, inadequate. However, from the remaining $2(N-M)$ adequate equations (M being the number of nodes on C_1), one can solve the relations (a matrix form) between the fields of the outermost nodes and of the next-to-outermost nodes (the nodes on C_2 in Fig. 1). Once such relations are solved, the explicit relations between associated fields (H_x and H_y) and their normal derivatives at the boundary of the inhomogeneous region can be deduced in a simple manner.

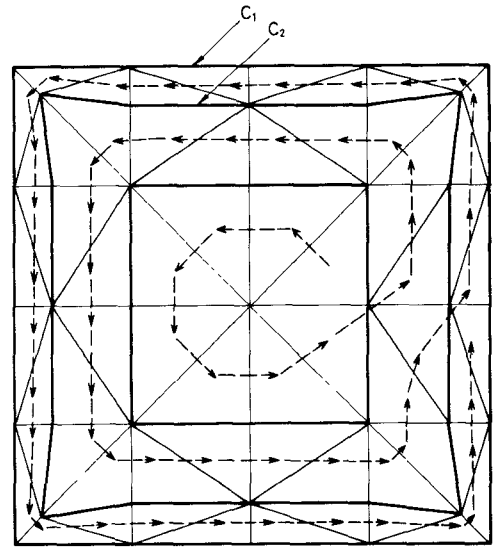

Fig. 1. Configuration and ordering of the elements in a frontal solution. The dashed arrows indicate the ordering of elements in the assembling/elimination process.

In employing the finite-element technique, one obtains a sparse matrix. The conventional Gauss elimination procedure results in a great waste of core storage. This problem is avoided by employing the frontal algorithm [17], [18]. The concept of the frontal algorithm is that the Gauss eliminations with respect to the fields of some nodes are made in the process of matrix assembling as soon as the assembling for that node is completed. Thus, those rows pertaining to that node can be deleted. If one would like to construct the entire field patterns, such matrix elements can be stored in a secondary storage device for later use in back-substitution. Thereby, the matrix size is proportional to the square of the number of nodes on the boundary rather than proportional to the square of the number of entire nodes.

With the aim of obtaining the relations between the fields of the outermost and of the next-to-outermost nodes, the assembling/elimination process starts from the innermost elements and then moves outward gradually, as indicated in Fig. 1. After the last element is treated, a matrix equation with a size of $2M\times 4M$ (for convenience, the nodes on C_2 is made normal to C_1 and the number of nodes on C_2 is made equal to M, as depicted in Fig. 1) in the fields of the outermost and the next-to-outermost nodes emerges, from which the explicit relations for the inhomogeneous region can be deduced and the propagation characteristics can be obtained (see Section II).

It is noted that for a given region and elements, the effective bandwidth in the present elimination process is larger than that in the method employing the artificial zero boundary or infinite elements. However, the actual region to be manipulated by the finite-element in the combined method is much smaller than those in the other two methods, especially in treating the propagation constants close to cutoff or in handling coupled waveguides.

V. Results

In this investigation, we use triangular elements and expand all the associated fields in linear basis functions. In treating isolated waveguides, no symmetry property was used. In treating two identical coupled waveguides, symmetry about the plane bisecting the two waveguides was utilized such that the inhomogeneous region to be manipulated by the finite-element is the same as in the case of the corresponding isolated waveguide.

To examine the accuracy of the proposed method, we compare the results of a rotational symmetric waveguide with the parabolic profile ($a = b$ in (8)), as shown in Fig. 2. For such a special case, highly accurate methods are available, such as in [16]. From Fig. 2, it is seen that the agreement between the results is quite good. At a high normalized propagation constant B (defined below), the fields concentrate in the core region, and, accordingly, the variations of the fields become stronger. This fact accounts for the accuracy of the calculated results being worse for a high B value. Similarly, it can be expected that the accuracy is worse for higher modes since the field variations of such modes become larger.

In the following, we consider coupled and uncoupled elliptical and diffusion waveguides. The results are presented in normalized frequency V_s and normalized propagation constant B, where

$$V_s = 2k_0 b(\epsilon_g - \epsilon_2)^{1/2}/\pi$$

and

$$B = \left[(\beta/k_0)^2 - \epsilon_2\right]/(\epsilon_g - \epsilon_2).$$

The notation of H^y_{mn} (H^x_{mn}) designates that mode for which the dominant magnetic field is directed in the $y(x)$ direction and the dominant field pattern has m and n peaks in the x and y directions, respectively.

A. Elliptical Waveguide

The elliptical waveguide considered has a parabolic profile, i.e.,

$$\epsilon(x, y) = \epsilon_g - (\epsilon_g - \epsilon_2)\left(\frac{x^2}{a^2} + \frac{y^2}{b^2}\right), \qquad \text{for } \frac{x^2}{a^2} + \frac{y^2}{b^2} \leq 1$$

$$= \epsilon_2, \qquad \text{elsewhere.} \tag{8}$$

Dispersion curves of such a waveguide with $a/b = 2$ and a permittivity ratio ϵ_r ($= \epsilon_g/\epsilon_2$) of 2.25 are shown in Fig. 3. The corresponding scalar solutions ($\epsilon_r \to 1$) are shown in Fig. 4. Comparing Figs. 3 and 4, it is seen that the curves of the H^x_{mn} modes deviate more than those of the H^y_{mn} modes as the permittivity ratio ϵ_r is increased. Such a situation is also found in homogeneous rectangular waveguide [14], [19]. Cutoff frequencies of some lower modes are presented in Table I. It is seen that there are two fundamental modes H^y_{11} and H^x_{11} for such a guiding structure. Dispersion curves of the corresponding coupled waveguides (directional coupler) are illustrated in Figs. 5 and 6, where the separation s is the distance between the two centers of the ellipses minus the length of the major axes. Similar to homogeneous coupled waveguides [14], each mode of the corresponding isolated waveguide is split into two modes. For such split modes, the pattern of H_y is either even (the H^x_{mne} or the H^y_{mne} mode) or odd (the H^x_{mno} or the H^y_{mno} mode) with respect to the plane of symmetry. Comparing Figs. 5 and 6, it is seen that, using normalized quantities, the magnitudes of splitting do not depend much on the permittivity ratio. From Figs. 5 and 6, it is evident that the splitting is stronger for a smaller propagation

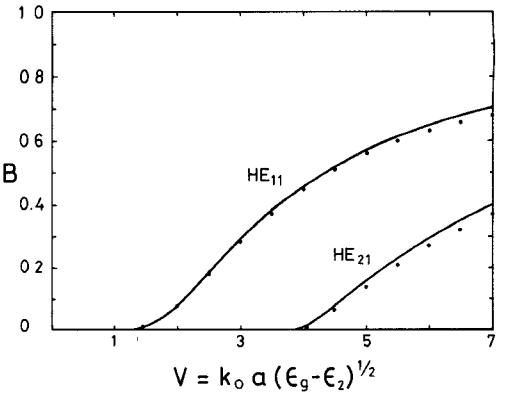

Fig. 2. Dispersion curves of a circular waveguide with the parabolic profile and with $\epsilon_g/\epsilon_2 = 2.25$. The solid line is taken from [16], which may be deemed as exact; the dots correspond to the proposed method with the number of nodes $N_n = 121$ and the number of elements $N_e = 210$.

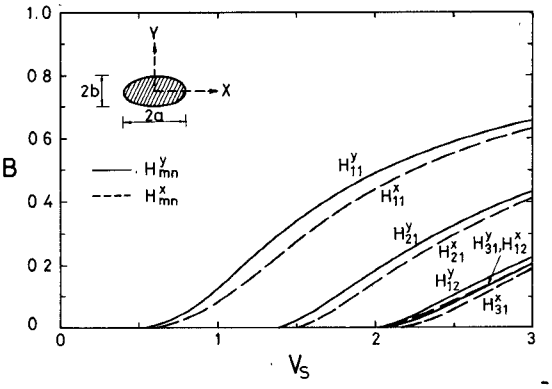

Fig. 3. Vectorial dispersion curves of the elliptical waveguide. $N_n = 121$ and $N_e = 210$.

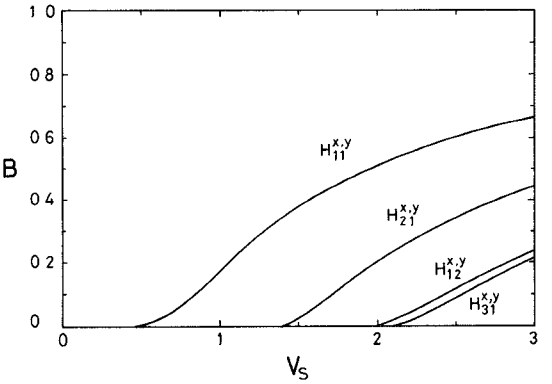

Fig. 4. Scalar dispersion curves of the elliptical waveguide.

TABLE I
NORMALIZED CUTOFF FREQUENCIES OF THE ELLIPTICAL WAVEGUIDE

			coupled waveguides, s=b			
	$\epsilon_r \to 1$	$\epsilon_r = 2.25$	$\epsilon_r \to 1$		$\epsilon_r = 2.25$	
Mode			even	odd	even	odd
H_{11}^y	0.00	0.00	0.00	0.704	0.00	0.766
H_{11}^x	0.00	0.00	0.704	0.00	0.831	0.00
H_{21}^y	1.403	1.388	1.362	1.477	1.340	1.471
H_{21}^x	1.403	1.524	1.477	1.362	1.596	1.483
H_{31}^y	2.044	2.013	2.037	2.192	2.005	2.188
H_{31}^x	2.044	2.129	2.192	2.037	2.286	2.125
H_{12}^y	1.997	2.045	1.967	2.028	2.016	2.075
H_{12}^x	1.997	2.013	2.028	1.967	2.053	1.971

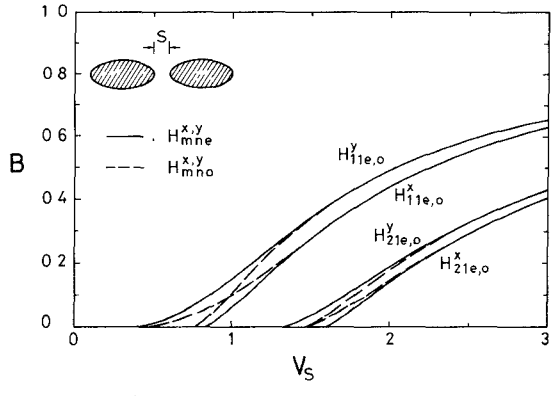

Fig. 5. Vectorial dispersion curves of two identical, coupled elliptical waveguides.

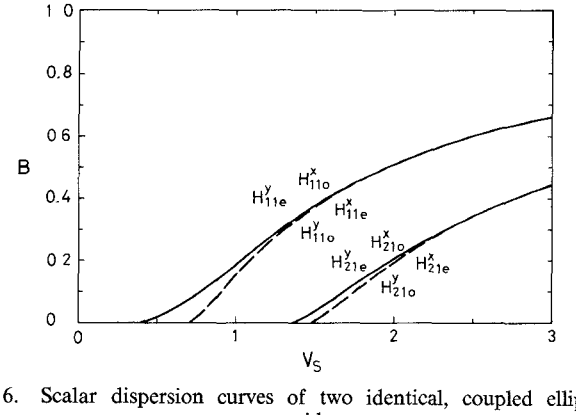

Fig. 6. Scalar dispersion curves of two identical, coupled elliptical waveguides.

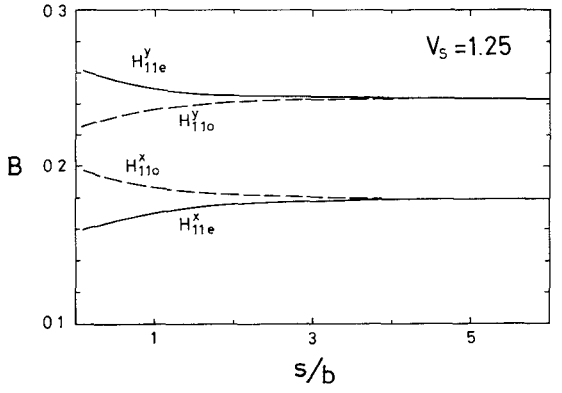

Fig. 7. Splitting of the fundamental modes of the elliptical waveguide as a function of separation s.

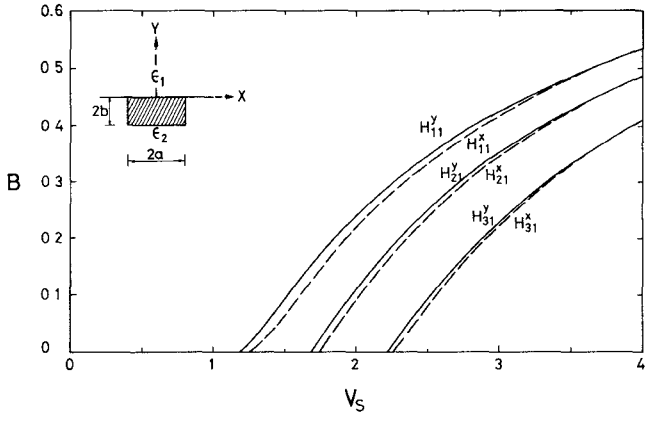

Fig. 8. Dispersion curves of the diffusion waveguide with $a/b = 2$, $D/b = 1$, $\epsilon_g/\epsilon_1 = 2.25$, and $\epsilon_2/\epsilon_1 = 2.15$. $N_n = 136$ and $N_e = 232$.

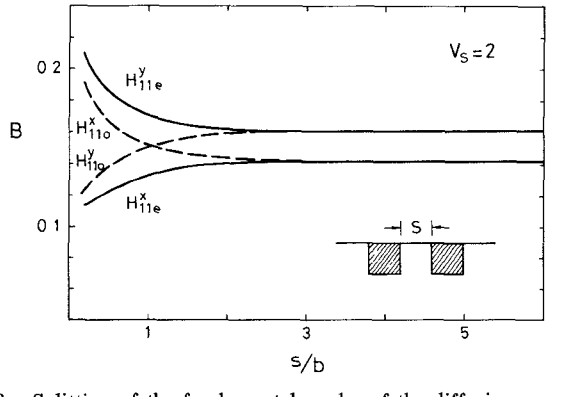

Fig. 9. Splitting of the fundamental modes of the diffusion waveguide with $a/b = 1$, $D/b = 1$, $\epsilon_g/\epsilon_1 = 2.25$, and $\epsilon_2/\epsilon_1 = 2.15$ as a function of separation s. $N_n = 82$ and $N_e = 136$.

constant B or for lower modes, which indicates that under such situations the fields penetrate farther away from the core regions. When the coupled waveguides are operated at a high propagation constant, no substantial coupling can be expected.

Cutoff frequencies of coupled waveguides are also presented in Table I. It is found that the cutoff frequency of one split mode (from either fundamental mode) shifts from zero, and the other split mode is never cutoff. Again, the entire guiding structure possesses two fundamental modes H_{11e}^y and H_{11o}^x. The separation s of coupled waveguides has a strong effect on the coupling coefficient as shown in Fig. 7. Note that, for given values of B and V_s, the explicit relations (between the fields and their normal derivatives) for the inhomogeneous regions are identical, regardless of how far the coupled waveguides are separated. Thereby, considerable computation effort can be saved if one treats several couplers with different separations s simultaneously, as in constructing Fig. 7.

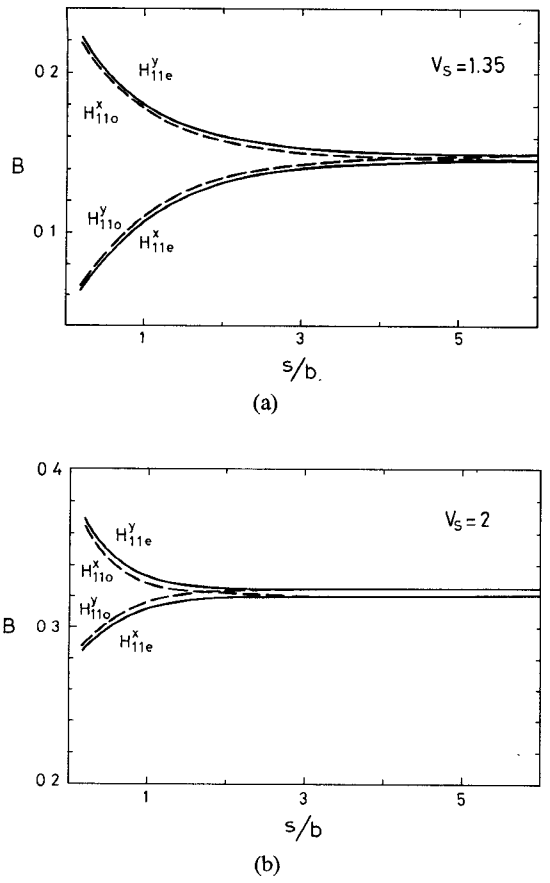

Fig. 10. Splitting of the fundamental modes of the diffusion waveguide with $a/b = 1$, $D/b = 1$, $\epsilon_g/\epsilon_1 = 2.25/2.15$, and $\epsilon_2/\epsilon_1 = 1$ as a function of separation s. (a) $V_s = 1.35$. (b) $V_s = 2$.

B. Diffusion Waveguide

The diffusion waveguides considered have a Gaussian profile, i.e.,

$$\epsilon(x, y) = \epsilon_2 + (\epsilon_g - \epsilon_2)\exp\left[-(y/D)^2\right], \quad \text{for } |x| \leqslant a, 0 \geqslant y \geqslant -2b$$
$$= \epsilon_1, \quad \text{for } y > 0$$
$$= \epsilon_2, \quad \text{elsewhere} \tag{9}$$

which models the permittivity distribution of a homogeneous substrate (with relative permittivity ϵ_2) processed by a masked one-dimensional diffusion. Dispersion curves of the first six modes of such a guiding structure are shown in Fig. 8. It is seen that the curves of the H^x_{mn} and the H^y_{mn} modes come together as in the channel waveguide discussed in [15], for which the inhomogeneous region is replaced by a homogeneous one. However, the discrepancy between such two modes is larger for the diffusion waveguide. This phenomenon is due partly to the fact that the permittivity of the inhomogeneous region is made large at the substrate surface, where, as a consequence, the fields become stronger than in the corresponding channel waveguide ($D \to \infty$). Since the permittivity discontinuity at the surface is large and the fields are not negligible there, a larger discrepancy between the H^x_{mn} and the H^y_{mn} modes is expected.

Similar splitting due to mutual coupling also exists in the coupled diffusion waveguides as shown in Figs. 9 and 10. Comparing Figs. 9 and 10(a), it is seen that, for the same range of B and the same separation s, the coupling coefficient (the magnitude of splitting in B) in Fig. 9 is much weaker than the corresponding coupler with an increased ϵ_1 (Fig. 10(a)). This fact is accounted for by noting that the permittivity of the air (ϵ_1) in Fig. 9 is much smaller than that of the substrate (ϵ_2). Consequently, the fields are more confined in the core regions, which in turn results in a smaller coupling coefficient. From such results, it seems plausible to enhance the coupling coefficients by coating the coupled diffusion waveguides with a dielectric layer of a higher permittivity. However, from Fig. 10(b), it is noted that, for a given frequency, such an enhancement will be compensated since the coupler is also driven to a higher B when ϵ_1 is increased.

VI. Conclusions

A combined method employing both the finite-element technique and the surface integral equations method is proposed, and has been used to analyze propagation characteristics of coupled and uncoupled elliptical and diffusion waveguides. Cutoff frequencies of isolated and coupled elliptical waveguides are also presented. Since this combined method does not suffer from the appearance of spurious modes, it is convenient in the analysis of new guiding structures.

Acknowledgment

The author is grateful to Dr. Shyh-Kang Jeng for the suggestion of employing the frontal algorithm.

References

[1] Z. J. Csendes and P. Silvester, "Numerical solution of dielectric loaded waveguides: I—Finite-element analysis," *IEEE Trans. Microwave Theory Tech.*, vol. MTT-18, pp. 1124–1131, Dec. 1970.

[2] M. Ikeuchi, H. Sawami, and H. Niki, "Analysis of open-type dielectric waveguides by the finite-element iterative method," *IEEE Trans. Microwave Theory Tech.*, vol. MTT-29, pp. 234–239, Mar. 1981.

[3] N. Mabaya, P. E. Lagasse, and P. Vandenbulcke, "Finite element analysis of optical waveguides," *IEEE Trans. Microwave Theory Tech.*, vol. MTT-29, pp. 600–605, June 1981.

[4] K. Oyamada and T. Okoshi, "Two-dimensional finite-element method calculation of propagation characteristics of axially nonsymmetrical optical fibers," *Radio Sci.*, vol. 17, pp. 109–116, 1982.

[5] B. M. A. Rahman and J. B. Davies, "Finite-element analysis of optical and microwave waveguide problems," *IEEE Trans. Microwave Theory Tech.*, vol. MTT-32, pp. 20–28, Jan. 1984.

[6] ——, "Penalty function improvement of waveguide solution by finite element," *IEEE Trans. Microwave Theory Tech.*, vol. MTT-32, pp. 922–928, Aug. 1984.

[7] C. Yeh, S. B. Dong, and W. Oliver, "Arbitrarily shaped inhomogeneous optical fiber of integrated optical waveguides," *J. Appl. Phys.*, vol. 46, pp. 2125–2129, May 1975.

[8] C. Yeh, K. Ha, S. B. Dong, and W. P. Brown, "Single-mode optical waveguides," *Appl. Opt.*, vol. 18, pp. 1490–1504, May 1979.

[9] C. C. Su, "Origin of spurious modes in the analysis of dielectric waveguides using the finite-difference or finite-element technique," *Electron. Lett.*, vol. 21, pp. 858–860, Sept. 1985.

[10] C. G. Williams and G. K. Cambrell, "Numerical solution of surface waveguide modes using transverse field components," *IEEE Trans. Microwave Theory Tech.*, vol. MTT-22, pp. 329–330, Mar. 1974.

[11] J. Katz, "Novel solution of 2-D waveguides using the finite-element method," *Appl. Opt.*, vol. 21, pp. 2747–2750, Aug. 1982.
[12] A. Konrad, "Vector variational formulation of electromagnetic fields in anisotropic media," *IEEE Trans. Microwave Theory Tech.*, vol. MTT-24, pp. 553–559, Sept. 1976.
[13] M. Koshiba, K. Hayata, and M. Suzuki, "Approximate scalar finite-element analysis of anisotropic optical waveguides with off-diagonal elements in a permittivity tensor," *IEEE Trans. Microwave Theory Tech.*, vol. MTT-32, pp. 587–593, June 1984.
[14] C. C. Su "A surface integral equations method for homogeneous optical fibers and coupled image lines of arbitrary cross-sections," *IEEE Trans. Microwave Theory Tech.*, vol. MTT-33, pp. 1114–1119, Nov. 1985.
[15] ——, "Analysis of versatile dielectric waveguides using the surface integral equations method," submitted for publication.
[16] C. C. Su and C. H. Chen, "Calculation of propagation constants and cutoff frequencies of radially inhomogeneous optical fiber," *IEEE Trans. Microwave Theory Tech.*, vol. MTT-34, pp. 328–332, Mar. 1986.
[17] B. M. Irons, "A frontal solution program for finite element analysis," *Int. J. Num. Meth. Eng.*, vol. 2, pp. 5–32, 1970.
[18] P. Hood, "Frontal solution program for unsymmetric matrices," *Int. J. Num. Meth. Eng.*, vol. 10, pp. 379–399, 1979.
[19] J. E. Goell, "A circular-harmonic computer analysis of rectangular dielectric waveguide," *Bell Syst. Tech. J.*, vol. 48, pp. 2133–2160, Sept. 1969.

✠

Ching-Chuan Su was born in Taiwan on October 2, 1955. He received the B.S., M.S., and Ph.D. degrees in electrical engineering from National Taiwan University in 1978, 1980, and 1985, respectively.

From 1980 to 1982, he was employed in an IC company, where he was responsible for the development of several MOS fabrication processes. In 1985, he joined the faculty of National Tsing Hua University, Hsinchu, Taiwan, where he currently serves as an Associate Professor in electrical engineering. His theoretical interests include bistability in nonlinear optics, and numerical methods in dielectric waveguide, body scattering, and MOS device simulation.